

A Generalized Scalarization Method for Evolutionary Multi-Objective Optimization

Ruihao Zheng, Zhenkun Wang*

School of System Design and Intelligent Manufacturing, Southern University of Science and Technology, Shenzhen, China
12132686@mail.sustech.edu.cn, wangzhenkun90@gmail.com

Abstract

The decomposition-based multi-objective evolutionary algorithm (MOEA/D) transforms a multi-objective optimization problem (MOP) into a set of single-objective subproblems for collaborative optimization. Mismatches between subproblems and solutions can lead to severe performance degradation of MOEA/D. Most existing mismatch coping strategies only work when the L_∞ scalarization is used. A mismatch coping strategy that can use any L_p scalarization, even when facing MOPs with non-convex Pareto fronts, is of great significance for MOEA/D. This paper uses the global replacement (GR) as the backbone. We analyze how GR can no longer avoid mismatches when L_∞ is replaced by another L_p with $p \in [1, \infty)$, and find that the L_p -based ($1 \leq p < \infty$) subproblems having inconsistently large preference regions. When p is set to a small value, some middle subproblems have very small preference regions so that their direction vectors cannot pass through their corresponding preference regions. Therefore, we propose a generalized L_p (GL_p) scalarization to ensure that the subproblem's direction vector passes through its preference region. Our theoretical analysis shows that GR can always avoid mismatches when using the GL_p scalarization for any $p \geq 1$. The experimental studies on various MOPs conform to the theoretical analysis.

Introduction

The multi-objective optimization problem (MOP) can be written as

$$\begin{aligned} & \text{minimize} && \mathbf{f}(\mathbf{x}) = (f_1(\mathbf{x}), \dots, f_m(\mathbf{x}))^\top, \\ & \text{subject to} && \mathbf{x} \in \Omega, \end{aligned} \quad (1)$$

where $\mathbf{x} = (x_1, \dots, x_n)^\top$ is a decision vector (also called solution), and $\Omega \subset \mathbb{R}^n$ denotes the decision space. $\mathbf{f} : \mathbb{R}^n \rightarrow \mathbb{R}^m$ is composed of m objective functions, and $\mathbf{f}(\mathbf{x})$ is the objective vector corresponding to \mathbf{x} .

The multi-objective evolutionary algorithm based on decomposition (MOEA/D) is a popular framework for dealing with MOPs (Zhang and Li 2007). It converts an MOP into a set of single-objective subproblems to optimize them simultaneously. The subproblem function is defined by a scalarization method, where the family of the L_p ($p \geq 1$) scalarization is often used. The weighted sum (WS) method and

the Tchebycheff (TCH) method are the L_1 scalarization and the L_∞ scalarization, respectively. Any scalarization method can be used in MOEA/D, and each has its own strengths and weaknesses (Hansen 2000; Wang, Zhang, and Zhang 2016).

In MOEA/D, each subproblem is associated with one solution. For each iteration, the evolutionary operations are conducted with respect to each subproblem to generate a new solution; this new solution is used to replace several neighboring subproblems' original solutions if it is better than these solutions. As stated in (Wang et al. 2014; Li et al. 2014), there may exist mismatches between solutions and subproblems and the above replacement strategy can lead to severe performance degradation. Sequentially, several MOEA/D variants with mismatch coping strategies have been proposed, such as MOEA/D-GR (Wang et al. 2014), MOEA/D-STM (Li et al. 2014), MOEA/D-IR (Li et al. 2015), MOEA/D-AMOSTM (Wu et al. 2017), and MOEA/D-2TCHMFI (Ma et al. 2018). Most of these algorithms employ the TCH method to define subproblems. Because the TCH-based subproblem has a good property, *i.e.*, the intersection between its direction vector and the Pareto front is optimal for it. Nevertheless, the TCH method has some specific weaknesses compared to other L_p scalarization methods. It is non-smooth, non-differentiable, and may cause slow convergence of MOEA/D, making it difficult to use in many scenarios. Therefore, it is of great significance for MOEA/D to develop mismatch coping strategies that enable using any L_p scalarization method, even when facing MOPs with non-convex Pareto fronts.

This paper adopts MOEA/D-GR as the backbone. It matches the most suitable subproblem for each new solution according to the function values over all subproblems. Our analysis first reveals that MOEA/D-GR can avoid mismatches only when the TCH method (*i.e.*, L_∞) is used. When the TCH method is replaced with another L_p scalarization for any $p \in [1, \infty)$, MOEA/D-GR fails to choose the appropriate subproblem for each solution. For example, MOEA/D-GR always chooses boundary subproblems to update if the TCH method is substituted with the WS method. Our analysis demonstrates that these mismatches can be attributed to L_p -based ($1 \leq p < \infty$) subproblems having inconsistently large preference regions. When p is set to a small value, the corresponding subproblems have preference regions with extremely imbalanced sizes. The boundary sub-

*Corresponding author.

problem's preference region is much larger than that of the middle subproblem (as shown in Figure 2). Such an imbalance leads to severe mismatches in MOEA/D-GR.

To fill this gap, we propose a generalized L_p (GL_p) scalarization for the subproblem definition. The GL_p -based subproblems can have uniform preference regions, no matter what the value of p ($p \geq 1$) is set to. We apply the GL_p scalarization to MOEA/D-GR and term the new algorithm as MOEA/D-GGR. The effectiveness of MOEA/D-GGR is validated with different p -values on various continuous and combinatorial MOPs. The results indicate that our method can avoid mismatches using the scalarization of any norm (*i.e.*, p can be $1, 2, \dots, \infty$), even in dealing with MOPs with non-convex or other complex Pareto fronts. Our method significantly expands the applicability of MOEA/D.

Background

Basic Concepts

Definition 1. For two objective vectors $\mathbf{u} = (u_1, \dots, u_m)^\top$ and $\mathbf{v} = (v_1, \dots, v_m)^\top$, \mathbf{u} is said to **dominate** \mathbf{v} , if $u_i \leq v_i$ for all $i \in \{1, \dots, m\}$ and $u_j < v_j$ for at least one $j \in \{1, \dots, m\}$.

Definition 2. \mathbf{x}^* is called the **Pareto optimal solution**, if there is no $\mathbf{x} \in \Omega$ such that $\mathbf{f}(\mathbf{x})$ dominates $\mathbf{f}(\mathbf{x}^*)$. Correspondingly, $\mathbf{f}(\mathbf{x}^*)$ is called the **non-dominated vector**.

Definition 3. The set of all Pareto optimal solutions is called the **Pareto set** (denoted as PS), and its image in the objective space is called the **Pareto front** (denoted as PF).

Definition 4. The **ideal point** $\mathbf{z}^{ide} = (z_1^{ide}, \dots, z_m^{ide})^\top$ is defined as $z_i^{ide} = \min\{f_i(\mathbf{x}) | \mathbf{x} \in \Omega\}$, for $i = 1, \dots, m$.

Definition 5. The **utopian point** $\mathbf{z}^{uto} = (z_1^{uto}, \dots, z_m^{uto})^\top$ is defined as $z_i^{uto} = z_i^{ide} - \varepsilon_i$, for $i = 1, \dots, m$, where $\varepsilon_i > 0$ is a relatively small computationally significant scalar.

L_p Scalarization

The L_p scalarization defines the single-objective optimization subproblem as

$$g^p(\mathbf{x} | \mathbf{w}, \mathbf{z}^*) = \left(\sum_{i=1}^m (w_i |f_i(\mathbf{x}) - z_i^*|)^p \right)^{\frac{1}{p}}, \quad (2)$$

where $\mathbf{w} = (w_1, \dots, w_m)^\top$ is a weight vector that satisfies $w_i \geq 0$ for each $i \in \{1, \dots, m\}$ and $\sum_{i=1}^m w_i = 1$. The reference vector $\mathbf{z}^* = (z_1^*, \dots, z_m^*)^\top$ is usually set to \mathbf{z}^{ide} . By using a set of uniformly distributed weight vectors $\{\mathbf{w}^j\}_{j=1}^N$ in Eq. (2), N single-objective subproblems can be achieved.

Let $\mathbf{z}^* = \mathbf{z}^{ide}$ and $p = 1$, Eq. (2) can be simplified as

$$g^{ws}(\mathbf{x} | \mathbf{w}, \mathbf{z}^*) = \sum_{i=1}^m w_i (f_i(\mathbf{x}) - z_i^*). \quad (3)$$

Eq. (3) is also known as the WS method. When $p \rightarrow \infty$, Eq. (2) can be written as

$$g^{tch}(\mathbf{x} | \mathbf{w}, \mathbf{z}^*) = \max_{i \in \{1, \dots, m\}} w_i (f_i(\mathbf{x}) - z_i^*). \quad (4)$$

Eq. (4) is also known as the TCH method. For any Pareto optimal solution \mathbf{x}^* , there exists a weight vector such that

\mathbf{x}^* is the optimal solution of the corresponding TCH-based subproblem (Miettinen 2012). For the subproblem defined by Eq. (4) with a weight vector \mathbf{w}^j , we refer $\boldsymbol{\lambda}^j = (\frac{1}{w_1^j}, \dots, \frac{1}{w_m^j})^\top$ to as its direction vector. The intersection between $\boldsymbol{\lambda}^j$ and the PF is the optimal objective vector of this subproblem (Qi et al. 2014).

MOEA/D Framework

MOEA/D employs N uniformly distributed weight vectors $\{\mathbf{w}^j\}_{j=1}^N$ to generate N subproblems. MOEA/D calculates the Euclidean distance between every two subproblems' weight vectors and uses these distances to define the mating and replacement neighborhoods for each subproblem. MOEA/D maintains a population with N solutions $\mathbf{x}^1, \dots, \mathbf{x}^N$, where \mathbf{x}^j is associated with the j -th subproblem for $j = 1, \dots, N$. The mating or replacement neighborhood of \mathbf{x}^j (denoted as B_m^j or B_r^j) consists of the solutions of the j -th subproblem's the T_m or T_r closest neighbors. At each iteration, MOEA/D conducts operations with respect to the j -th subproblem for each $j \in \{1, \dots, N\}$ as follows:

- Conduct reproduction operators on solutions randomly selected from B_m^j to generate a new solution \mathbf{x}^{new} .
- For each solution \mathbf{x}^k of B_r^j , replace \mathbf{x}^k by \mathbf{x}^{new} if \mathbf{x}^{new} is better than it.

GR

In MOEA/D, the new solution is only allowed to update the solutions of the neighboring subproblems. As shown in Figure 1, the new solution of the 4-th subproblem is only allowed to update the 4-th subproblem's three neighboring subproblems' solutions (*i.e.*, solutions of the 3-rd to the 5-th subproblems). However, this replacement may cause mismatches between subproblems and solutions, thereby severely hindering the algorithm's performance. For example, the new solution in Figure 1 cannot benefit the neighbors of the 4-th subproblem but can facilitate the convergence of the 7-th and 8-th subproblems.

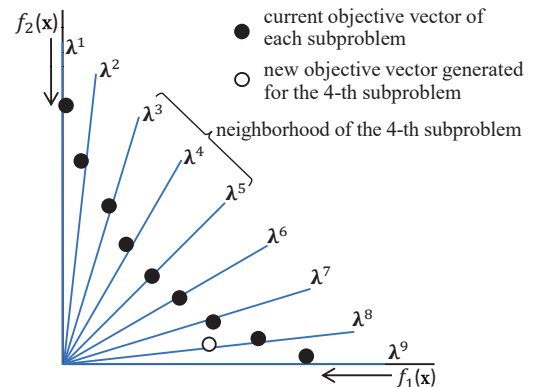


Figure 1: A case of mismatch in MOEA/D.

GR globally selects suitable updating subproblems for each new solution. For the new solution \mathbf{x}^{new} , GR first lo-

ates the most appropriate subproblem via

$$j = \arg \min_{k \in \{1, \dots, N\}} \{g^{tch}(\mathbf{x}^{new} | \mathbf{w}^k, \mathbf{z}^*)\}. \quad (5)$$

Thereafter, the solutions of subproblems within the neighborhood of the j -th subproblem are assigned to \mathbf{x}^{new} for updating. Since MOEA/D-GR utilizes the new solution's subproblem function values to determine its most appropriate subproblem, the choice of the scalarization method that defines the subproblem function is critical.

Generalized L_p Scalarization

Motivation

According to (Ma et al. 2018), the preference region of the j -th subproblem can be described as

$$\Upsilon^j = \left\{ \mathbf{f}(\mathbf{x}) | \mathbf{x} \in \Omega, \arg \min_{k \in \{1, \dots, N\}} \{g(\mathbf{x} | \mathbf{w}^k, \mathbf{z}^*)\} = j \right\}. \quad (6)$$

The preference regions of the L_p -based subproblems are illustrated in Figure 2. When $p = 1$, only the 1-st and 7-th subproblems have the preference regions and the other subproblems show no preference region. When $p = 2$, all the subproblems have preference regions, but some subproblems' direction vectors (e.g., $\lambda^2, \lambda^3, \lambda^5, \lambda^6$) do not pass through their corresponding regions.

Definition 6. A subproblem is called **boundary subproblem** if \mathbf{w} has at least one minimal entry. A subproblem is called **extreme boundary subproblem** if \mathbf{w} has $(m - 1)$ minimal entries.

Theorem 1. For L_1 -based subproblems, only the extreme boundary subproblems have preference regions.

Proof. Without loss of generality, we assume $z_i^* = 0$, $f_i \in \mathbb{R}_{\geq 0}$ and $w_i \in \mathbb{R}_{\geq 0}$ for $i = 1, \dots, m$. The subproblem of a given preference objective vector \mathbf{f} can be determined by solving the following linear programming problem

$$\begin{aligned} & \underset{\mathbf{w}}{\text{minimize}} && \mathbf{w}^\top \mathbf{f}, \\ & \text{subject to} && \begin{cases} A\mathbf{w} = b, \\ w_i \geq 0 \text{ for } i = 1, \dots, m, \end{cases} \end{aligned} \quad (7)$$

where $A = [1 \dots 1]^{1 \times m}$ and $b = 1$. The optimal solution to this problem is one of the basic solutions. Denote B_k as k -th column of A . Since $B_k^{-1}b = 1$ for $k = 1, \dots, m$, then the basic solution k to this problem is

$$w_i^{bas_k} = \begin{cases} 1, & i = k, \\ 0, & i \neq k. \end{cases} \quad (8)$$

Eq. (8) represents that the subproblem of a given preference objective vector \mathbf{f} is always one of the extreme boundary subproblems. \square

Theorem 2. The direction vectors of L_p -based ($1 \leq p < \infty$) subproblems are not guaranteed to pass through the corresponding preference regions except direction vector $(m, \dots, m)^\top$. The direction vectors of L_∞ -based subproblems all pass through the corresponding preference regions. \square

Proof. We assume $z_i^* = 0$, $f_i \in \mathbb{R}_{\geq 0}$ and $w_i \in \mathbb{R}_{\geq 0}$ for $i = 1, \dots, m$. $\sum_{i=1}^m w_i = 1$ is substituted into Eq. (2) and then we have

$$g'(\mathbf{w} | \mathbf{f}, \mathbf{z}^*) = \left(\sum_{i=1}^{m-1} (w_i f_i)^p + \left(1 - \sum_{i=1}^{m-1} w_i \right)^p f_m^p \right)^{\frac{1}{p}}. \quad (9)$$

The first-order partial derivative of Eq. (9) with respect to w_k is

$$\frac{\partial g'(\mathbf{w} | \mathbf{f}, \mathbf{z}^*)}{\partial w_k} = \sigma_1 \cdot \sigma_2, \quad (10)$$

where

$$\begin{aligned} \sigma_1 &= \frac{1}{p} \left(\sum_{i=1}^{m-1} (w_i f_i)^p + \left(1 - \sum_{i=1}^{m-1} w_i \right)^p f_m^p \right)^{\frac{1}{p}-1}, \\ \sigma_2 &= p \left(w_k^{p-1} f_k^p - \left(1 - \sum_{i=1}^{m-1} w_i \right)^{p-1} f_m^p \right). \end{aligned} \quad (11)$$

$\frac{\partial g'(\mathbf{w} | \mathbf{f}, \mathbf{z}^*)}{\partial w_k} = 0$ if and only if $\sigma_1 = 0$ or $\sigma_2 = 0$. First, let $\sigma_1 = 0$, we can get $w_i f_i = 0$ for $i = 1, \dots, m$. Since $w_i \geq 0$ and $f_i \geq 0$, w_i or f_i must be 0. σ_2 in this case must be 0. Secondly, let $\sigma_2 = 0$, we can obtain

$$w_k^{p-1} f_k^p = \left(1 - \sum_{i=1}^{m-1} w_i \right)^{p-1} f_m^p. \quad (12)$$

According to Eq. (12), the solution satisfies

$$\left(\frac{w_k}{w_i} \right)^{p-1} = \left(\frac{f_i}{f_k} \right)^p, \quad i, k \in \{1, \dots, m\}. \quad (13)$$

Then the solution can be written as

$$w_i = \left(\frac{1}{\alpha f_i} \right)^{\frac{p}{p-1}}, \quad \text{for } i = 1, \dots, m, \quad (14)$$

where $\alpha \geq 0$ is a constant that ensure $\sum_{i=1}^m w_i = 1$. There exists $A \in \mathbb{R}^{m \times m}$ and $b \in \mathbb{R}^m$ which are

$$A = \begin{bmatrix} 1 & 0 & \dots & \dots & 0 \\ 0 & 1 & & & 0 \\ \vdots & & \ddots & & \vdots \\ 0 & & & 1 & 0 \\ -1 & \dots & \dots & -1 & 0 \end{bmatrix}, \quad (15)$$

$$b = (0, \dots, 0, 1)^\top,$$

such that

$$g^{lp}(A\mathbf{w} + b | \mathbf{f}, \mathbf{z}^*) = g'(\mathbf{w} | \mathbf{f}, \mathbf{z}^*). \quad (16)$$

Since $g^{lp}(\mathbf{w} | \mathbf{f}, \mathbf{z}^*)$ is a norm as well as a convex function, Eq. (9) is a convex function. Then, Eq. (14) is a global minimal solution.

Eq. (14) can be rewritten as $\frac{1}{w_i} = (\alpha f_i)^{\frac{p}{p-1}}$ for $i = 1, \dots, m$. If we have infinitely sampled weight vectors, each subproblem's preference region is a line. When $p \rightarrow \infty$, $\frac{1}{w_i} = \alpha f_i$. The corresponding subproblem's direction vector passes through its preference region. When p takes a value from $(1, \infty)$, only direction vector $(m, \dots, m)^\top$ passes through its preference region while other direction vectors cannot pass through their corresponding preference regions. \square

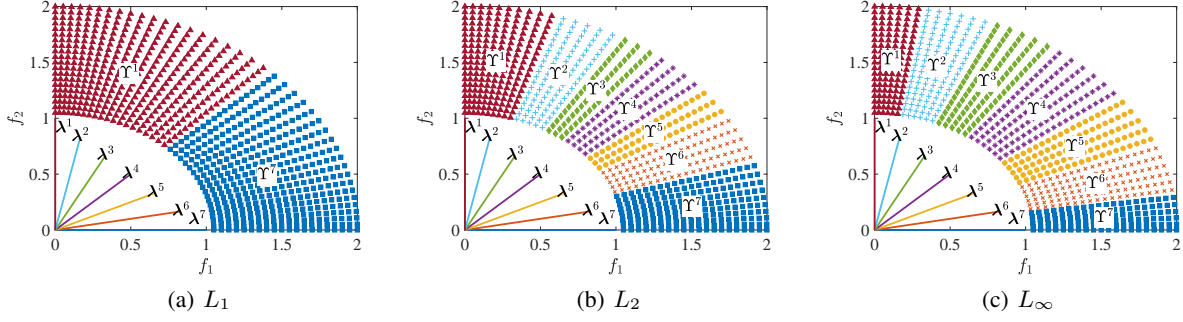


Figure 2: Preference regions of L_p -based subproblems with $\mathbf{z}^* = (0, 0)^\top$ and $\{\mathbf{f} = (f_1, f_2)^\top | 1 \leq \|\mathbf{f}\|_2 \leq 2\}$.

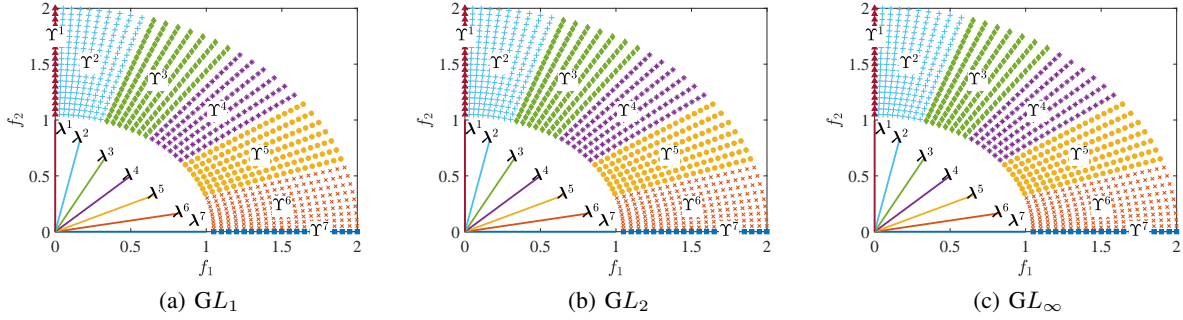


Figure 3: Preference regions of GL_p -based subproblems with $\mathbf{z}^* = (0, 0)^\top$ and $\{\mathbf{f} = (f_1, f_2)^\top | 1 \leq \|\mathbf{f}\|_2 \leq 2\}$.

Theorems 1 and 2 demonstrate that the L_p scalarization with $p \in [1, \infty)$ can cause the performance deterioration of MOEA/D-GR. As shown in Figure 4, many objective vectors obtained by MOEA/D-GR (L_1) are far away from the PF . Theorem 1 indicates that MOEA/D-GR (L_1) always selects one of the boundary subproblems for a new solution. As a result, the other subproblems cannot be selected for updating. Figure 4 also shows that MOEA/D-GR (L_∞) has a better population uniformity than MOEA/D-GR (L_2). According to Theorem 2, the L_p scalarization with $p \in [1, \infty)$ causes mismatches in MOEA/D-GR and makes MOEA/D-GR fail to achieve a good population uniformity.

The significance of the above analysis is by no means limited to explaining the mismatches in MOEA/D-GR. As argued in (Hao, Liu, and Wang 2017), some mismatches are incurred when MOEA/D-GR (L_∞) adopts \mathbf{z}^{uto} instead of \mathbf{z}^{ide} as the reference vector. The reasons can be inferred using Theorem 2 as well. If the boundary subproblems exceed the feasible objective space, boundary subproblems are never selected for updating in MOEA/D-GR. Moreover, other newly proposed scalarization methods (Jiang et al. 2018) can also use this analysis of the preference regions to validate if they can deal with mismatches well.

Methodology

The idea of the GL_p scalarization is to modify the L_p scalarization such that any direction vector of a subproblem can pass through its corresponding preference region. The GL_p

scalarization is formulated as

$$g^{glp}(\mathbf{x}|\mathbf{w}, \mathbf{z}^*) = \left(\sum_{i=1}^m (w_i (f_i(\mathbf{x}) - z_i^*))^p \right)^{\frac{1}{p}} \cdot h(\mathbf{w}), \quad (17)$$

where $h(\mathbf{w})$ enables the GL_p scalarization to satisfy the requirement. Note that $h(\mathbf{w})$ only changes the scale of $g^{glp}(\mathbf{x}|\mathbf{w}, \mathbf{z}^*)$ among different \mathbf{w} . $h(\mathbf{w})$ is a constant for a particular \mathbf{w} , and thus the contour shape remains the same. Moreover, the computational effort is low since $h(\mathbf{w})$ can be pre-calculated for each subproblem.

We assume $z_i^* = 0$, $f_i \in \mathbb{R}_{\geq 0}$ and $w_i \in \mathbb{R}_{\geq 0}$ for $i = 1, \dots, m$, the first-order partial derivative of $g^{glp}(\mathbf{w}|\mathbf{f}, \mathbf{z}^*)$ with respect to w_k can be calculated as

$$\frac{\partial g^{glp}(\mathbf{w}|\mathbf{f}, \mathbf{z}^*)}{\partial w_k} = \left(\sum_{i=1}^m (w_i f_i)^p \right)^{\frac{1}{p}-1} w_k^{p-1} f_k^p h(\mathbf{w}) + \left(\sum_{i=1}^m (w_i f_i)^p \right)^{\frac{1}{p}} \frac{\partial h(\mathbf{w})}{\partial w_k}. \quad (18)$$

Let $w_i = \frac{1}{\alpha f_i}$ for $i = 1, \dots, m$ such that $\frac{\partial g^{glp}(\mathbf{w}|\mathbf{f}, \mathbf{z}^*)}{\partial w_k} = 0$, we can obtain

$$\frac{\partial h(\mathbf{w})}{\partial w_k} = -\frac{1}{m w_k} h(\mathbf{w}). \quad (19)$$

According to Eq. (19), $h(\mathbf{w})$ can be

$$h(\mathbf{w}) = \exp \left(-\frac{1}{m} \ln \prod_{i=1}^m w_i \right) = \left(\prod_{i=1}^m w_i \right)^{-\frac{1}{m}}. \quad (20)$$

Theorem 3. *The direction vectors of GL_p -based ($p \geq 1$) subproblems all pass through the corresponding preference regions.*

Proof. We assume $z_i^* = 0$, $f_i \in \mathbb{R}_{\geq 0}$ and $w_i \in \mathbb{R}_{\geq 0}$ for $i = 1, \dots, m$. Let $w_i = \frac{1}{\alpha f_i} + v_i t$ for $i = 1, \dots, m$ where \mathbf{v} is any vector and $t \geq 0$, we have

$$g^{glp}(\mathbf{w}|\mathbf{f}, \mathbf{z}^*) = g'(t) = \left(\sum_{i=1}^m \left(\frac{1}{\alpha} + v_i f_i t \right)^p \right)^{\frac{1}{p}} \cdot h'(t), \quad (21)$$

where

$$h'(t) = \exp \left(-\frac{1}{m} \sum_{i=1}^m \ln \left(\frac{1}{\alpha f_i} + v_i t \right) \right). \quad (22)$$

The first-order derivative of Eq. (21) is

$$\frac{\partial g'(t)}{\partial t} = \sigma_3 (\sigma_4 - \sigma_5), \quad (23)$$

where

$$\begin{aligned} \sigma_3 &= h'(t) \left(\sum_{i=1}^m \left(\frac{1}{\alpha} + v_i f_i t \right)^p \right)^{\frac{1}{p}-1}, \\ \sigma_4 &= \sum_{i=1}^m \left(\frac{1}{\alpha} + v_i f_i t \right)^{p-1} v_i f_i, \\ \sigma_5 &= \frac{1}{m} \sum_{i=1}^m \left(\frac{1}{\alpha} + v_i f_i t \right)^p \sum_{i=1}^m \frac{v_i}{\frac{1}{\alpha f_i} + v_i t}. \end{aligned} \quad (24)$$

First, we consider the sign of $\sigma_4 - \sigma_5$. Since $v_i = \frac{1}{t} (w_i - \frac{1}{\alpha f_i})$, we have

$$\begin{aligned} \sigma_4 &= \sum_{i=1}^m v_i w_i^{p-1} f_i^p, \\ \sigma_5 &= \sum_{i=1}^m \left(\frac{w_i}{m} \sum_{j=1}^m \frac{v_j}{w_j} \right) w_i^{p-1} f_i^p, \\ v_i &= \left(\frac{w_i}{m} \sum_{j=1}^m \frac{v_j}{w_j} \right) = \frac{w_i}{t} \left(\frac{1}{m} \sum_{j=1}^m \frac{1}{\alpha f_j w_j} - \frac{1}{\alpha f_i w_i} \right). \end{aligned} \quad (25)$$

Then

$$\begin{aligned} \sigma_4 - \sigma_5 &= \frac{1}{\alpha t} \sum_{i=1}^m (w_i f_i)^p \left(\frac{1}{m} \sum_{j=1}^m \frac{1}{f_j w_j} - \frac{1}{f_i w_i} \right) \\ &= \frac{1}{\alpha t} \left(\frac{1}{m} \sum_{i=1}^m (w_i f_i)^p \sum_{i=1}^m \frac{1}{w_i f_i} - \sum_{i=1}^m (w_i f_i)^p \frac{1}{w_i f_i} \right). \end{aligned} \quad (26)$$

We can assume $w_1 f_1 \geq \dots \geq w_m f_m$, $\tilde{w}_1 \tilde{f}_1 \leq \dots \leq \tilde{w}_m \tilde{f}_m$ and $w_i f_i = \tilde{w}_{m-i+1} \tilde{f}_{m-i+1}$ for $i = 1, \dots, m$. According to

rearrangement inequality and Tchebycheff's sum inequality, the following inequality holds

$$\begin{aligned} \sigma_4 - \sigma_5 &\geq \frac{1}{\alpha t} \left(\frac{1}{m} \sum_{i=1}^m (w_i f_i)^p \sum_{i=1}^m \frac{1}{w_i f_i} - \sum_{i=1}^m (w_i f_i)^p \frac{1}{\tilde{w}_i \tilde{f}_i} \right) \\ &\geq \frac{1}{\alpha t} \left(\frac{1}{m} \sum_{i=1}^m (w_i f_i)^p \sum_{i=1}^m \frac{1}{w_i f_i} - \frac{1}{m} \sum_{i=1}^m (w_i f_i)^p \sum_{i=1}^m \frac{1}{\tilde{w}_i \tilde{f}_i} \right) = 0. \end{aligned} \quad (27)$$

Since $\frac{1}{\alpha} + v_i f_i t = w_i f_i \geq 0$, $\sigma_3 \geq 0$. Therefore, Eq. (23) ≥ 0 which represents that $g^{glp}(\mathbf{w}|\mathbf{f}, \mathbf{z}^*)$ is unimodal. Let $\sigma_3 = 0$, we can get $w_i f_i = \frac{1}{\alpha} + v_i f_i t = 0$ for $i = 1, \dots, m$. In this case, $\sigma_4 = 0$ and $\sigma_5 = 0$. $\sigma_4 - \sigma_5 = 0$ if and only if $w_i f_i = w_j f_j$, $i, j \in \{1, \dots, m\}$. Then the global minimal solution is $w_i = \frac{1}{\alpha f_i}$ for $i = 1, \dots, m$. \square

The preference regions of the GL_p -based subproblems are illustrated in Figure 3. In the 2-objective case, the preference regions are almost the same regardless of how p -value varies. But the preference region sizes of boundary subproblems are quite small. To cope with this problem, MOEA/D-GGR¹ is proposed. The difference between MOEA/D-GGR and MOEA/D-GR is the scalarization method and the replacement neighborhood. After determining the replacement neighborhood as MOEA/D-GR does, each boundary subproblem is added to the neighborhood of the closest non-boundary subproblem in MOEA/D-GGR. This modification makes each boundary subproblem's solution have a higher updating probability without degrading the preference regions of other subproblems.

Experimental Studies

Experimental Setup

Test Instances. We use ZDT1-ZDT4 (Zitzler, Deb, and Thiele 2000), DTLZ1, DTLZ3 and DTLZ5 (Deb et al. 2005), the multi-objective knapsack problem (MOKP) (Zitzler and Thiele 1999), and the multi-objective traveling salesman problem (MOTSP) (Corne and Knowles 2007) to verify the algorithm performance. We set the decision vector dimension to 30, 30, 30 and 10 for ZDT1-ZDT4 respectively, and to $(m + 4)$ for each DTLZ instance. The MOKP instances are randomly generated with 250 items. The MOTSP instances are randomly generated with 60 vertices. Each solution is encoded by real numbers for the ZDT and DTLZ instances, by binary numbers for MOKP, and by a permutation for MOTSP.

General Algorithm Settings. MOEA/D and MOEA/D-GR are compared with MOEA/D-GGR. All the algorithms are implemented on the PlatEMO platform (Tian et al. 2017). The detailed parameter settings are as follows:

¹<https://github.com/EricZheng1024/MOEA-D-GGR>

Problem	m	I_H	$p = 1$			$p = 2$			$p \rightarrow \infty$		
			MOEA/D	MOEA/D-GR	MOEA/D-GGR	MOEA/D	MOEA/D-GR	MOEA/D-GGR	MOEA/D	MOEA/D-GR	MOEA/D-GGR
ZDT1	2	mean	0.8614(2)-	0.0097(3)-	0.8657(1)	0.871(1)+	0.8398(3)-	0.869(2)	0.8655(3)-	0.8699(1)=	0.8698(2)
		std.	7.4e-04	2.3e-02	4.0e-03	2.0e-04	5.9e-03	2.1e-03	2.0e-03	2.2e-03	1.9e-03
ZDT2	2	mean	0.21(2)-	0(3)-	0.4436(1)	0.5174(1)=	0.4507(3)-	0.5108(2)	0.5327(3)-	0.5343(2)=	0.5348(1)
		std.	7.4e-12	0.0e+00	4.0e-02	2.6e-03	4.4e-02	1.4e-02	1.6e-03	6.7e-03	6.2e-03
ZDT3	2	mean	0.4873(2)-	0.03427(3)-	0.7154(1)	0.6826(2)-	0.6824(3)-	0.719(1)	0.7173(3)-	0.7215(2)-	0.7217(1)
		std.	9.6e-02	3.7e-02	2.2e-03	3.7e-02	2.6e-02	1.6e-03	1.2e-02	3.7e-03	3.8e-03
ZDT4	2	mean	0.845(2)=	0(3)-	0.8487(1)	0.8599(2)=	0.8051(3)-	0.8599(1)	0.8431(3)-	0.8566(2)=	0.857(1)
		std.	1.2e-02	0.0e+00	8.8e-03	5.2e-03	4.8e-02	4.8e-03	1.4e-02	8.5e-03	9.4e-03
DTLZ1	2	mean	0.2099(2)-	0(3)-	0.7027(1)	0.7025(2)-	0.6875(3)-	0.7041(1)	0.7045(3)-	0.7049(2)=	0.7049(1)
		std.	1.3e-04	0.0e+00	1.6e-03	2.9e-04	1.3e-04	7.2e-05	3.8e-04	1.6e-04	1.7e-04
	3	mean	0.4923(2)-	0.2171(3)-	1.033(1)	1.115(1)+	1.078(3)-	1.113(2)	1.101(1)+	1.1(2)=	1.1(3)
		std.	7.6e-02	1.8e-01	8.3e-03	2.2e-04	7.9e-04	2.1e-04	6.3e-04	2.9e-04	2.0e-04
	5	mean	0.8878(2)-	0.7822(3)-	1.318(1)	1.511(3)-	1.519(1)+	1.516(2)	1.511(3)-	1.513(1)+	1.512(2)
std.		1.2e-01	3.8e-01	6.3e-02	7.1e-04	4.0e-03	2.2e-03	9.9e-04	1.3e-03	1.6e-03	
DTLZ3	2	mean	0.2099(2)-	0.00818(3)-	0.4138(1)	0.2099(3)-	0.4164(2)-	0.4171(1)	0.4197(3)-	0.42(1)=	0.42(2)
		std.	2.1e-04	2.1e-02	1.8e-02	7.5e-05	1.1e-02	1.2e-04	3.4e-04	1.1e-04	2.1e-04
	3	mean	0.3307(2)-	0.1788(3)-	0.6244(1)	0.3317(3)-	0.6016(2)-	0.6508(1)	0.7344(1)+	0.733(2)=	0.7329(3)
		std.	3.9e-04	1.4e-01	5.6e-03	4.0e-03	8.8e-03	5.2e-03	1.3e-03	7.3e-04	7.9e-04
	5	mean	0.6102(2)-	0.5385(3)-	0.6111(1)	0.6208(3)-	0.6493(2)-	0.8244(1)	1.146(3)-	1.149(1)=	1.148(2)
std.		1.1e-03	4.6e-02	8.9e-04	1.7e-02	7.3e-02	6.6e-02	1.1e-03	3.0e-03	2.2e-03	
DTLZ5	3	mean	0.131(3)-	0.161(2)-	0.232(1)	0.131(3)-	0.2246(2)-	0.2331(1)	0.2644(1)+	0.2556(3)-	0.2559(2)
		std.	3.2e-10	9.4e-03	9.8e-04	6.6e-06	1.5e-03	1.6e-03	4.1e-06	1.4e-05	5.1e-05
	5	mean	0.1464(3)-	0.1524(1)+	0.1481(2)	0.1464(3)-	0.1475(2)-	0.1504(1)	0.1925(1)+	0.15(3)-	0.1894(2)
		std.	5.0e-04	4.0e-03	1.6e-03	4.1e-04	2.5e-03	1.6e-03	5.1e-04	1.0e-03	4.2e-04
MOKP	2	mean	0.8719(2)=	0.2195(3)-	0.8748(1)	0.8731(1)=	0.8227(3)-	0.8691(2)	0.8384(3)-	0.8503(1)=	0.8495(2)
		std.	1.1e-02	9.3e-02	8.8e-03	8.8e-03	1.4e-02	9.5e-03	1.3e-02	1.2e-02	1.2e-02
	3	mean	0.6274(2)-	0.1097(3)-	0.6561(1)	0.6588(2)-	0.636(3)-	0.6657(1)	0.6239(3)-	0.636(2)=	0.6366(1)
		std.	1.1e-02	2.2e-02	6.1e-03	7.2e-03	7.1e-03	6.5e-03	7.1e-03	5.6e-03	5.4e-03
MOTSP	2	mean	0.9733(2)-	0.03373(3)-	0.9852(1)	0.9815(2)=	0.9491(3)-	0.9861(1)	0.9392(3)-	0.9679(2)=	0.9711(1)
		std.	1.5e-02	4.7e-02	1.0e-02	1.1e-02	1.5e-02	9.5e-03	1.2e-02	1.2e-02	1.4e-02
	3	mean	0.9253(2)=	0.2679(3)-	0.929(1)	0.9016(2)-	0.8854(3)-	0.9131(1)	0.8174(3)-	0.8503(1)=	0.8452(2)
		std.	1.3e-02	3.8e-02	1.1e-02	1.4e-02	1.2e-02	1.1e-02	1.5e-02	1.6e-02	1.7e-02
Total +/-/=		0/13/3	1/15/0	\	2/10/4	1/15/0	\	4/12/0	1/3/13	\	

Table 1: Mean and standard deviation of I_H metric values. The rank of each algorithm on each instance is provided after the mean of the I_H metric value. +, - or = denotes that the performance of the corresponding algorithm is statistically better than, worse than or similar to that of MOEA/D-GGR based on Wilcoxon’s rank sum test at 0.05 significant level.

- The population size N : 100 ($m = 2$) or 190 ($m = 3$).
- The maximal number of function evaluations: 25000 for ZDT1-ZDT4, 100000 for DTLZ1, DTLZ3 and DTLZ5, 200000 for 2-objective MOKP and MOTSP, and 400000 for 3-objective MOKP and MOTSP.
- The number of independent runs: 30 for each instance.
- The neighborhood size: $T_m = 0.1N$ and $T_r = \lceil 0.05N \rceil$.
- Reproduction operators: For real number coding, the simulated binary crossover (SBX) and polynomial mutation (PM) are used (Purshouse and Fleming 2007). The SBX control parameters p_c , η_c and p_e are set to 1, 20 and 0, respectively. The PM control parameters p_m and η_m are set to $1/n$ and 20, where n is the number of decision variables. For binary coding, the uniform crossover and bit-flip mutation are used (Syswerda 1989). The crossover rate is 1; the mutation rate is $2/n$ for a bit. For

permutation coding, the order-based crossover and simple inversion mutation are used (Larranaga et al. 1999). The crossover rate is 1 and the mutation rate is 0.1.

Performance Metric. The hypervolume indicator (I_H) is used to assess the performance of each algorithm (Zitzler and Thiele 1999). Let P be an approximate solution set and $\mathbf{z}^h = (z_1^h, \dots, z_m^h)^\top$ be a reference objective vector. The I_H metric value is computed by

$$I_H(P, \mathbf{z}^h) = \text{vol} \left(\bigcup_{\mathbf{x} \in P} [f_1(\mathbf{x}), z_1^h] \times \dots \times [f_m(\mathbf{x}), z_m^h] \right), \quad (28)$$

where $\text{vol}(\cdot)$ is the Lebesgue measure. A larger I_H metric value indicates a better algorithm performance. Before calculate the I_H metric value, we normalize $\{f_i(\mathbf{x}) | \mathbf{x} \in P\}$ for $i = 1, \dots, m$ with the range from $\min\{f_i(\mathbf{x}) | \mathbf{x} \in PS\}$ to

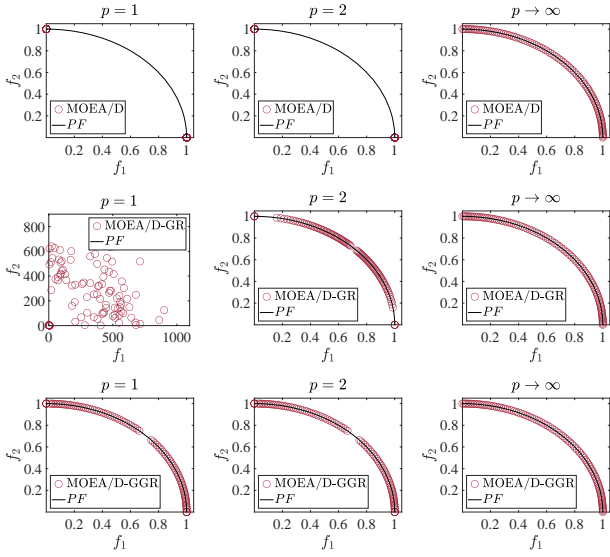


Figure 4: Plots of the objective vectors having the median I_H metric value obtained among each algorithm's 30 runs on 2-objective DTLZ3.

$\max\{f_i(\mathbf{x})|\mathbf{x} \in PS\}$. Then set $z_i^h = 1.1$ for $i = 1, \dots, m$. The PF s are unknown on the MOKP and MOTSP instances. Each of them is approximated by the set of all non-dominated solutions obtained by all algorithms in all runs.

Experimental Results

The I_H metric values obtained by the three algorithms on 16 test instances are given in Tables 1. Our theoretical analysis holds on the problem with many-objective (e.g., DTLZ1, DTLZ3 and DTLZ5 with 5 objectives), discrete objective space (e.g., MOKP and MOTSP), convex PF (e.g., ZDT1 and ZDT4), concave PF (e.g., ZDT2 and DTLZ3), linear PF (e.g., DTLZ1), discontinuous PF (e.g., ZDT3).

When $p \rightarrow \infty$, MOEA/D-GGR and MOEA/D-GR have similar performance; MOEA/D is slightly worse than the two algorithms. When $p = 2$, MOEA/D-GGR is better than the other competitors on most test problems. When $p = 1$, MOEA/D-GGR significantly outperforms MOEA/D and MOEA/D-GR on all test problems except 5-objective DTLZ5. This instance has a highly degenerate PF . The direction vectors have few intersections with such a PF , making our mismatch avoidance strategy ineffective.

Figure 4 plots the obtained final objective vectors which have the median I_H metric values from each algorithm's 30 runs on 2-objective DTLZ3. When $p = 1$, MOEA/D-GGR is the only algorithm that overcomes mismatches, which achieves a satisfactory approximation to the PF ; MOEA/D and MOEA/D-GR fail to approximate the PF . When $p = 2$, MOEA/D still can only obtain the two boundary objective vectors; the objective vectors obtained by MOEA/D-GR cover the middle part but miss some boundary parts of the PF ; MOEA/D-GGR yields the best approximation of the PF compared to the other two algorithms. When $p \rightarrow \infty$, the three algorithms have similar good performance.

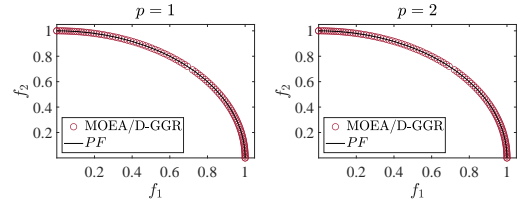


Figure 5: Plots of the objective vectors having the median I_H metric value obtained by MOEA/D-GGR ($p = 1$ and $p = 2$) using $T_r = 1$ on 2-objective DTLZ3.

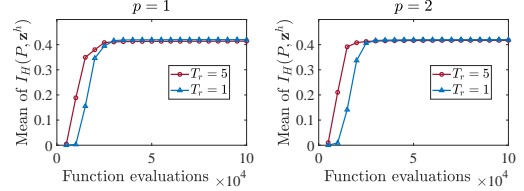


Figure 6: Evolution of the mean I_H metric values achieved by MOEA/D-GGR using two different T_r settings on 2-objective DTLZ3.

It is worth mentioning that the approximate set obtained by MOEA/D-GGR using GL_1 or GL_2 misses a small central part of the PF . It is because the diversity of MOEA/D-GGR is affected by the setting of T_r when GL_p with $1 \leq p < \infty$ is used. When a large T_r is adopted, MOEA/D-GGR using GL_p with $1 \leq p < \infty$ may miss some non-dominated objective vectors. In other words, its diversity can be improved by employing a small T_r . To validate it, we set T_r to 1 for MOEA/D-GGR with GL_1 and GL_2 and further test the two algorithms on the 2-objective DTLZ3. As shown in Figure 5, the obtained approximate set has much better diversity in both cases. But Figure 6 also indicates that a small T_r may discourage convergence. As reported in (Wang et al. 2016), a better approach is to adaptively change T_r during the search.

Overall, MOEA/D-GGR is less affected by the PF shape than MOEA/D and MOEA/D-GR.

Conclusion

In this paper, we have demonstrated that MOEA/D-GR still suffers from mismatches when the L_∞ scalarization is replaced by another L_p scalarization with $p \in [1, \infty)$. Our analysis reveals that this can be attributed to L_p -based ($1 \leq p < \infty$) subproblems having inconsistently large preference regions. When p is set to a small value, some middle subproblems have very small preference regions so that their direction vectors cannot pass through their corresponding preference regions. To fill this gap, we have proposed a new scalarization family called the GL_p scalarization. The GL_p -based subproblem's direction vector is guaranteed to pass through its corresponding preference region, which implies MOEA/D-GR can always avoid mismatches when using the GL_p scalarization for any $p \geq 1$. We have conducted various experimental studies to validate the effectiveness of the GL_p scalarization.

Acknowledgments

This work was supported in part by the National Natural Science Foundation of China under Grant 62106096; and in part by the Shenzhen Technology Plan under Grant JCYJ20220530113013031.

References

- Corne, D. W.; and Knowles, J. D. 2007. Techniques for highly multiobjective optimisation: some nondominated points are better than others. In *Proceedings of the 9th Annual Conference on Genetic and Evolutionary Computation (GECCO)*, 773–780.
- Deb, K.; Thiele, L.; Laumanns, M.; and Zitzler, E. 2005. Scalable test problems for evolutionary multiobjective optimization. In *Evolutionary Multiobjective Optimization*, 105–145. Springer.
- Hansen, M. P. 2000. Use of substitute scalarizing functions to guide a local search based heuristic: The case of moTSP. *Journal of Heuristics*, 6(3): 419–431.
- Hao, X.; Liu, J.; and Wang, Z. 2017. An improved global replacement strategy for MOEA/D on many-objective knapsack problems. In *2017 13th IEEE Conference on Automation Science and Engineering (CASE)*, 624–629. IEEE.
- Jiang, S.; Yang, S.; Wang, Y.; and Liu, X. 2018. Scalarizing functions in decomposition-based multiobjective evolutionary algorithms. *IEEE Transactions on Evolutionary Computation*, 22(2): 296–313.
- Larranaga, P.; Kuijpers, C. M. H.; Murga, R. H.; Inza, I.; and Dizdarevic, S. 1999. Genetic algorithms for the travelling salesman problem: A review of representations and operators. *Artificial Intelligence Review*, 13(2): 129–170.
- Li, K.; Kwong, S.; Zhang, Q.; and Deb, K. 2015. Interrelationship-based selection for decomposition multiobjective optimization. *IEEE Transactions on Cybernetics*, 45(10): 2076–2088.
- Li, K.; Zhang, Q.; Kwong, S.; Li, M.; and Wang, R. 2014. Stable matching-based selection in evolutionary multiobjective optimization. *IEEE Transactions on Evolutionary Computation*, 18(6): 909–923.
- Ma, X.; Zhang, Q.; Tian, G.; Yang, J.; and Zhu, Z. 2018. On Tchebycheff decomposition approaches for multiobjective evolutionary optimization. *IEEE Transactions on Evolutionary Computation*, 22(2): 226–244.
- Miettinen, K. 2012. *Nonlinear multiobjective optimization*, volume 12. Springer Science & Business Media.
- Purshouse, R. C.; and Fleming, P. J. 2007. On the evolutionary optimization of many conflicting objectives. *IEEE Transactions on Evolutionary Computation*, 11(6): 770–784.
- Qi, Y.; Ma, X.; Liu, F.; Jiao, L.; Sun, J.; and Wu, J. 2014. MOEA/D with adaptive weight adjustment. *Evolutionary Computation*, 22(2): 231–264.
- Syswerda, G. 1989. Uniform crossover in genetic algorithms. In *Proceedings of the 3rd International Conference on Genetic Algorithms (ICGA)*, 2–9.
- Tian, Y.; Cheng, R.; Zhang, X.; and Jin, Y. 2017. PlatEMO: A MATLAB platform for evolutionary multi-objective optimization [educational forum]. *IEEE Computational Intelligence Magazine*, 12(4): 73–87.
- Wang, R.; Zhang, Q.; and Zhang, T. 2016. Decomposition-based algorithms using Pareto adaptive scalarizing methods. *IEEE Transactions on Evolutionary Computation*, 20(6): 821–837.
- Wang, Z.; Zhang, Q.; Gong, M.; and Zhou, A. 2014. A replacement strategy for balancing convergence and diversity in MOEA/D. In *2014 IEEE Congress on Evolutionary Computation (CEC)*, 2132–2139. IEEE.
- Wang, Z.; Zhang, Q.; Zhou, A.; Gong, M.; and Jiao, L. 2016. Adaptive replacement strategies for MOEA/D. *IEEE Transactions on Cybernetics*, 46(2): 474–486.
- Wu, M.; Li, K.; Kwong, S.; Zhou, Y.; and Zhang, Q. 2017. Matching-based selection with incomplete lists for decomposition multiobjective optimization. *IEEE Transactions on Evolutionary Computation*, 21(4): 554–568.
- Zhang, Q.; and Li, H. 2007. MOEA/D: A multiobjective evolutionary algorithm based on decomposition. *IEEE Transactions on Evolutionary Computation*, 11(6): 712–731.
- Zitzler, E.; Deb, K.; and Thiele, L. 2000. Comparison of multiobjective evolutionary algorithms: Empirical results. *Evolutionary computation*, 8(2): 173–195.
- Zitzler, E.; and Thiele, L. 1999. Multiobjective evolutionary algorithms: a comparative case study and the strength Pareto approach. *IEEE Transactions on Evolutionary Computation*, 3(4): 257–271.